Liquid Crystals
Publication details, including instructions for authors and subscription information:
http://www.informaworld.com/smpp/title~content=t713926090

The influence of chirality on the difference in flexoelectric coefficients investigated in uniform lying helix, Grandjean and twisted nematic structures

P. S. Salter[a]; C. Kischka[a]; S. J. Elston[a]; E. P. Raynes[a]
[a] Department of Engineering Science, University of Oxford, Oxford, UK

First published on: 08 October 2009

To cite this Article Salter, P. S. , Kischka, C. , Elston, S. J. and Raynes, E. P.(2009) 'The influence of chirality on the difference in flexoelectric coefficients investigated in uniform lying helix, Grandjean and twisted nematic structures', Liquid Crystals, 36: 12, 1355 — 1364, First published on: 08 October 2009 (iFirst)
To link to this Article: DOI: 10.1080/02678290903233991
URL: http://dx.doi.org/10.1080/02678290903233991

Liquid Crystals,
Vol. 36, No. 12, December 2009, 1355–1364

Taylor & Francis
Taylor & Francis Group

The influence of chirality on the difference in flexoelectric coefficients investigated in uniform lying helix, Grandjean and twisted nematic structures

P.S. Salter*, C. Kischka, S.J. Elston and E.P. Raynes

Department of Engineering Science, University of Oxford, Parks Road, Oxford OX1 3PJ, UK

(22 April 2009; final form 4 August 2009)

Measurements of the difference in flexoelectric coefficients ($e_1 - e_3$), using the sign convention as originally defined by Meyer, are reported from three experiments employing the flexoelectro-optic effect in different geometries. The uniform lying helix (ULH) structure is used to measure the tilt angle of the liquid crystal director with respect to the helix axis for an applied electric field, in order to infer a value for ($e_1 - e_3$). Alternatively, measurements of the flexoelectric difference can be made by considering the transmission through a device with an in-plane electric field aligned in either the Grandjean structure for highly chiral materials, or a twisted nematic (TN) structure for largely achiral materials. The results from the Grandjean and ULH structures show the equivalence of the measurement techniques with helix axis either perpendicular or parallel to the substrates. Further comparison of these results with the measurement from the achiral TN device shows that the difference in flexoelectric coefficients displays no dependence on chirality, demonstrating that flexoelectricity is purely associated with splay and bend director deformations, as expected from symmetry considerations.

Keywords: nematic; flexoelectricity; chirality

1. Introduction

Flexoelectricity in liquid crystals has been a subject of interest since it was first proposed by Meyer in 1969 (*1*). A splay or bend deformation of the nematic director $\hat{\mathbf{n}}$ induces an associated flexoelectric polarisation $P_{flexo,}$, which can be defined as

$$\mathbf{P}_{\text{flexo}} = e_1(\nabla \cdot \hat{\mathbf{n}})\hat{\mathbf{n}} + e_3(\nabla \times \hat{\mathbf{n}}) \times \hat{\mathbf{n}}, \qquad (1)$$

where e_1 and e_3 are the splay and bend flexoelectric coefficients, respectively, and the sign convention originally defined by Meyer (*1*) has been adopted. The flexoelectric polarisation is assigned no dependence on the pseudo-scalar twist deformations of the director $\hat{\mathbf{n}} \cdot (\nabla \times \hat{\mathbf{n}})$, since there is no associated unique direction along which a polarisation may arise. Therefore P_{flexo} is expected to be independent of chirality by symmetry considerations (*2*).

An applied electric field can couple to the flexoelectric polarisation inducing a deformation of the liquid crystal director. The bulk torque on the director can be written as $\mathbf{\Gamma} = \hat{\mathbf{n}} \times \mathbf{h}$ where $\mathbf{h}$ is the bulk molecular field with a flexoelectric component of the form (*3*):

$$\mathbf{h}_{\text{flexo}} = (e_1 - e_3)[\mathbf{E}(\nabla \cdot \hat{\mathbf{n}}) - (\nabla\hat{\mathbf{n}})\mathbf{E}] - (e_1 + e_3)(\hat{\mathbf{n}} \cdot \nabla)\mathbf{E}. \qquad (2)$$

Hence the bulk flexoelectric torque on the director can be decomposed into contributions that relate to the difference ($e_1 - e_3$) or the sum ($e_1 - e_3$) of the flexoelectric coefficients. Therefore, it is often these combinations that tend to be measured experimentally rather than e_1 and e_3 being determined independently. Effects dependent on the sum are only present when there is a gradient in the electric field and effects dependent on the difference are only important if there is a gradient in the director $\hat{\mathbf{n}}$.

Measurements of the difference of flexoelectric coefficients can be made by considering the flexoelectro-optic effect observed in chiral nematic liquid crystals with an electric field applied perpendicular to the helix axis, first reported by Patel and Meyer in 1987 (*4*). The electric field induces a tilt of the molecular director with respect to the helix axis about the direction of the field, forming a director distortion with a flexoelectric polarisation parallel to the field. The magnitude of the electric field can be considered constant along the helix but there is a gradient in the director $\hat{\mathbf{n}}$, so from Equation (2) it can be seen that the subsequent flexoelectric effect is dependent on the difference of flexoelectric coefficients. In fact, Patel and Meyer (*4*) showed that a simple analytic treatment yields an expression for the tilt angle ϕ of the director planes with respect to the helix axis as

*Corresponding author. Email: patrick.salter@eng.ox.ac.uk

ISSN 0267-8292 print/ISSN 1366-5855 online

DOI: 10.1080/02678290903233991
http://www.informaworld.com

$$\tan\phi = \frac{(e_1 - e_3)E}{q(K_1 + K_3)}, \quad (3)$$

where E is the magnitude of the applied electric field, K_1 and K_3 are the splay and bend Frank elastic coefficients and $q = 2\pi/p$ is the magnitude of the helical wavevector, where p is the pitch length. The flexoelectro-optic effect in chiral liquid crystals can be realised in two contrasting device geometries (*5*): either in the uniform lying helix (ULH) structure, where the helix axis is homogeneously aligned parallel to the device substrates, with a transverse electric field (*4*) or in the Grandjean structure, where the helix axis is perpendicular to the substrates, with an in-plane electric field (*6*).

A chiral nematic liquid crystal material, with a pitch of the order of the wavelength of light λ, aligned in the ULH structure appears as a negative uniaxial slab with the optic axis perpendicular to the director planes of the molecules (*7*). If an electric field is applied between the device substrates, a rotation of the molecular planes by angle ϕ about the direction of the field creates a flexoelectric polarisation parallel to the field. This is manifest macroscopically as an in-plane rotation of the optic axis by an angle ϕ. For an applied electric field of magnitude E, the transmission of the device between crossed polarisers is given by (*8*)

$$I(E) = I_0 \sin^2[2\alpha_0 + 2\phi(E)] \sin^2\left(\frac{\pi\Delta n(E)d}{\lambda}\right), \quad (4)$$

where α_0 is the angle between the first polariser and the zero-field optic axis and Δn is the effective birefringence of the helix. As can be seen from Equation (3), the tangent of the molecular tilt angle ϕ is linearly dependent on the applied electric field and reverses for a field of opposite polarity. A measurement of the magnitude and direction of the tilt angle immediately yields the magnitude and sign of $(e_1 - e_3)$, provided that the elastic constants and pitch of the material are also known.

This method provides a straightforward measurement for $(e_1 - e_3)$ and has been used extensively (*8*, *9*), but has a few problems. It can be difficult to obtain the well-aligned monodomain ULH structure required for the measurement, since there is no simple device geometry that supports the ULH as an equilibrium state. Most standard devices form either the Grandjean (helix perpendicular to substrate) or focal conic structure (randomly oriented polydomains) as the ground state. An electric field can orient the helical axis parallel to the substrates for positive $\Delta\epsilon$ materials by coupling to the molecular dielectric anisotropy, in order to form the ULH. The process is not applicable for negative $\Delta\epsilon$ materials, where the transverse electric field has the effect of aligning the helix axis perpendicular to the substrates in the Grandjean texture. Further, in order to create a monodomain ULH sample a shearing of the cell substrates is often required to induce flow within the cell and uniformly align the helix axis in the plane of the device (*10*, *11*). The method is additionally limited since it is only relevant to highly chiral liquid crystals, meaning that it cannot be used for the measurement of $(e_1 - e_3)$ for long pitch or pure achiral materials. These materials have to be doped with a chiral agent that may potentially affect the flexoelectric behaviour.

More fundamentally there are several key assumptions made in the analytic model used in the derivation of Equation (3) which could cause error in the values obtained for $(e_1 - e_3)$. The model assumes that the liquid crystal under consideration has zero dielectric anisotropy, and that under an applied electric field the cholesteric maintains a uniform helical profile with a constant tilt ϕ along the entire pitch length. Including a non-zero dielectric anisotropy in the model, with associated distortion of the helix, has no effect on the relationship between the tilt angle and $(e_1 - e_3)$, but flexoelectricity does have the effect of raising the critical field for dielectric unwinding of the helix (*4*). However the influence of a non-uniform rotation of the director along the length of the helix is yet to be fully explored.

An alternative method has been developed recently for the determination of $(e_1 - e_3)$ in achiral nematic liquid crystals utilising the flexoelectro-optic effect (*12*, *13*). Measurements of the transmission of an oblique incidence laser beam through a twisted nematic (TN) device with in-plane electrodes can also be used to ascertain a value for $(e_1 - e_3)$. The TN structure can be considered as a quarter pitch of a helix with the in-plane electrodes providing an electric field perpendicular to the helix axis. Therefore, there is a flexoelectrically induced tilt of the director relative to the helix axis and the direction of the tilt depends on the field polarity, which can be observed by monitoring the transmission through the device. Values for $(e_1 - e_3)$ are obtained by fitting the experimental measurements of the transmission to results from a numerical model used to determine the director structure and transmission of the device for a particular applied voltage. The model employed does not rely on any of the assumptions used in the derivation of Equation (3), providing an advantage over the ULH method described above. However, the significant benefit in using this approach is its applicability to measurements of achiral and negative $\Delta\epsilon$ materials, while the TN structure employed is stable and easily aligned, in stark contrast to the ULH.

Here we extend the method for measurement of $(e_1 - e_3)$ in the TN structure to a multi-turn Grandjean structure for a range of materials doped to be highly chiral. Here $(e_1 - e_3)$ is also determined for the chiral mixtures by observing the flexoelectrically induced tilt of the optic axis in a ULH structure. The aim is to compare the results obtained from the Grandjean and ULH structures to demonstrate the equivalence of the measurements in the different geometries. The results are further compared with measurements of $(e_1 - e_3)$ for the pure achiral materials in the TN structure, in order to show that chirality has no effect on the value of $(e_1 - e_3)$.

2. Experiments

In a recent study a correlation was observed between flexoelectricity and dielectric anisotropy: materials having high $\Delta\epsilon$ also tending to have a high positive value for $(e_1 - e_3)$ (see (*14*)). Therefore, three materials displaying a range in magnitude of $\Delta\epsilon$ were chosen for the experiment: MDA 02 2419, E7 and TL 216, all supplied by Merck. Their parameter values are shown in Table 1 and it can be seen that they all have positive $\Delta\epsilon$ as required for the ULH measurements. All three materials are naturally achiral and hence applicable for the TN structure. For the chiral measurements in the ULH and Grandjean structures they were mixed with a small amount of the chiral agent R5011 (Merck) which has a large helical twisting power of around 100 μm^{-1} and induces right-handed chirality. Short-pitch and long-pitch mixtures were made for measurement, the short pitch containing about 2% w/w R5011 and the long-pitch mixture containing about 1% w/w R5011. The room-temperature pitch was measured using a visible/infrared spectrometer to find the selective reflection wavelength band. The material parameters and values of the chiral pitch for the mixtures used are listed in Table 1.

3. ULH structure with transverse electric field

3.1 Experiment

The formation of a high-quality monodomain ULH sample is essential if accurate measurements of $(e_1 - e_3)$ are to be made. However, as mentioned above, there is no simple device geometry that supports the ULH as the minimum energy state, and an electric field is required to orient the helix axis parallel to the surfaces. Hybrid aligned nematic (HAN) devices were used here, where one substrate provides homeotropic alignment while the other provides planar alignment. The planar substrate promotes a single alignment direction for the helix axis in the plane of the device (*15*). The ULH structure was induced by cooling the device from the isotropic to the cholesteric state with an applied square wave voltage of magnitude greater than that required for helix unwinding. At a temperature 2°C below the phase transition the voltage was reduced until the ULH started to form. In some cases the upper substrate of the device needed to be manually rubbed during the reduction of the voltage in order to induce flow in the cell to achieve a well-aligned sample. The cell was cooled to room temperature and measurements of the tilt angle made as a function of decreasing voltage.

The magnitude of the tilt angle ϕ was measured for each voltage by monitoring the optical transmission of the device placed between crossed polarisers. The azimuthal orientation (α_{+E}) is noted for which the intensity at positive applied electric field is the maximum observed $I(+E) = I_{\max}$. The device is then rotated until $I(-E) = I_{\max}$ and the orientation α_{-E} recorded. By inspection of Equation (4), it can be seen that $\alpha_{+E} - \alpha_{+E} = 2\phi$. Measurements of the tilt angle could be made to an accuracy of 0.1°. The sign of the tilt angle can be determined by considering the change in transmission for a positive rotation (defined as a right-handed screw in the direction of the positive electric field) of the device.

Table 1. Parameter values for the three liquid crystal materials used in the experiments. The values are used for the calculation of $(e_1 - e_3)$ from the optic axis tilt angle measurements in the ULH structure and to fit experimental transmission data to the theory for oblique laser beams incident on Grandjean and TN structures with in-plane electric fields. For the pure materials, the elastic constants and dielectric anisotropy are determined from a study of the Freedericksz transition in various geometries, while the birefringence is measured using an Abbé refractometer. The chiral pitch is shown for mixtures of the materials with approximately 1% w/w and approximately 2% w/w of the dopant R5011. The values of the pitch are calculated from selective reflection data for devices aligned in the Grandjean structure. All measurements were performed at room temperature.

Material	K_1 (pN)	K_2 (pN)	K_3 (pN)	$\Delta\epsilon$	Δn	p (nm) (+ 2%)	p (nm) (+ 1%)
MDA 02 2419	8.2	6.1	15.3	38.5	0.180	374	683
E7	10.7	6.5	16.0	13.7	0.233	450	825
TL 216	13.8	8.1	18.6	5.1	0.207	395	855

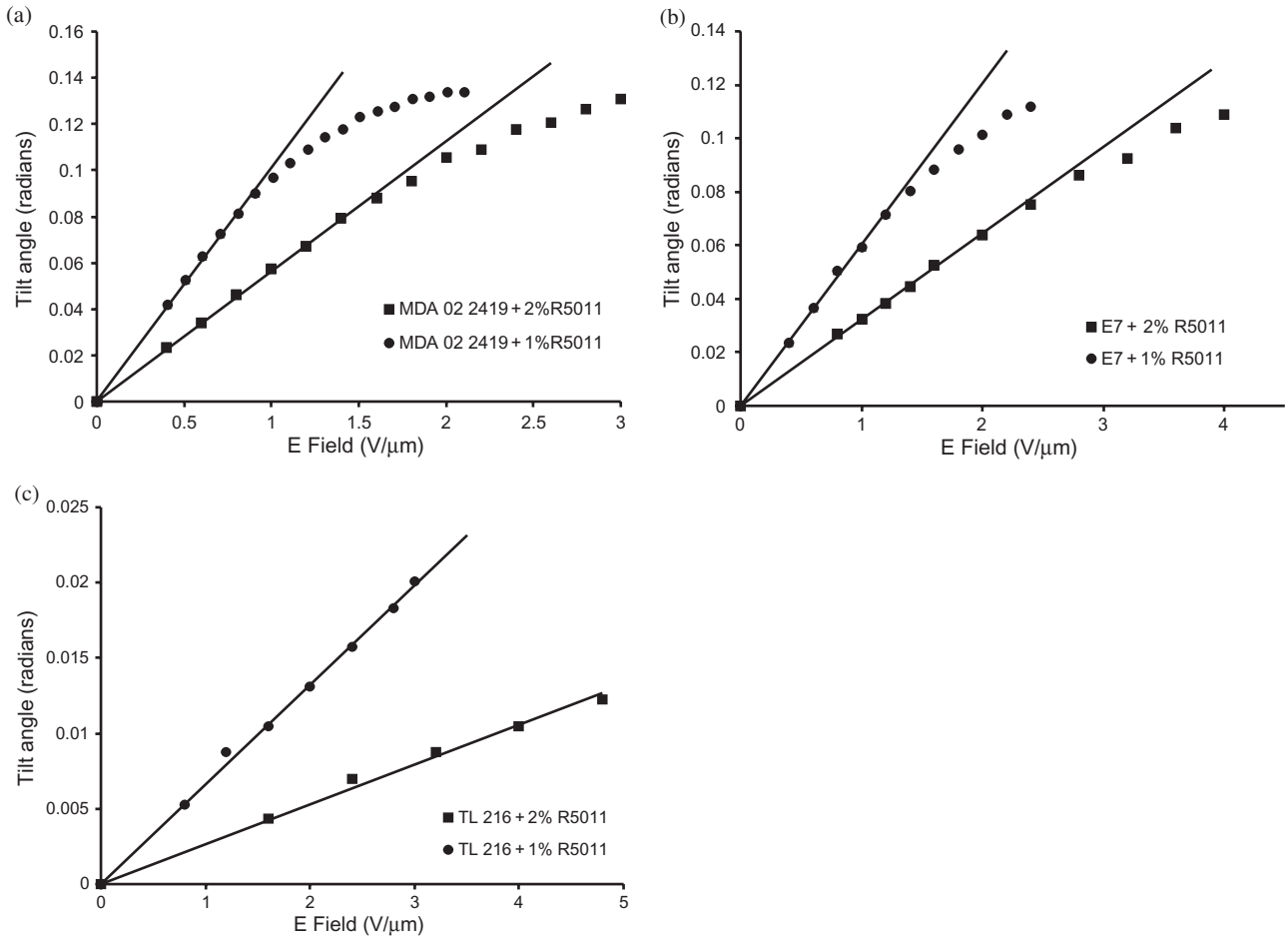

Figure 1. Measurements of the tilt angle ϕ of the optic axis in the ULH structure at room temperature for chiral mixtures of (a) MDA 02 2419, (b) E7 and (c) TL 216 as a function of the transverse electric field applied between the device substrates.

3.2 Results

Figure 1 shows measurements of the tilt angle ϕ of the optic axis as a function of applied electric field for the chiral mixtures of MDA 02 2419, E7 and TL 216 aligned in the ULH structure. The electric field was calculated by dividing the applied voltage by the cell gap, assuming that the ULH structure is uniform across the cell and the transition region from the surface alignment to the ULH bulk is small.

The tilt angle increases linearly with the applied field for small values of ϕ in accordance with Equation (3), for all three materials. Also the pitch dependence of the tilt angle ($\phi \propto p$) agrees well with Equation (3); for example, the two different chiral mixtures of the material MDA 02 2419 have gradients of ϕ against E in the linear regime of the data which differ by a factor of 0.56 while the pitch length ratio is 0.55. At higher electric fields the tilt angle is non-linear in the applied electric field and saturates for MDA 02 2419 and E7. Such an effect is attributed to the considerable distortion of the helix profile at high electric fields due to the coupling between the field and the dielectric anisotropy of the material. At fields close to that required for complete unwinding of the helix, the distortion of the helix is so great that the analytical treatment of the flexoelectro-optic effect breaks down. This interpretation is supported by the fact that the non-linearity is greatest for MDA 02 2419 which has the greatest $\Delta\epsilon$, while TL 216 shows minimal non-linearity and has the lowest value of $\Delta\epsilon$.

It is possible to extract values for $(e_1 - e_3)$ from the gradient of the graph for tilt angle against electric field in the linear regime, using Equation (3) combined with the values of K_1 and K_3 for the material given in Table 1. The results are given in Table 2 with an estimation of the associated error margin, related to uncertainty in the measurement of the flexoelectric tilt angle ϕ and also combined with a degree of uncertainty in the measurement of the parameters K_1, K_3 and p.

Table 2. Values of the difference in flexoelectric coefficients for the three materials obtained from measurements in the ULH, chiral Grandjean and achiral TN device geometries.

Material	ULH (pC m^{-1})	Chiral Grandjean (pC m^{-1})	Achiral TN (pC m^{-1})
MDA 02 2419	21.9 ± 1.5 ($p = 683$ nm) 22.2 ± 1.5 ($p = 374$ nm)	28.2 ± 4.0 ($p = 683$ nm)	22.0 ± 1.0
E7	12.3 ± 0.8 ($p = 825$ nm) 12.0 ± 0.8 (p = 450 nm)	12.2 ± 2.0 ($p = 825$ nm)	12.2 ± 1.0
TL 216	1.57 ± 0.3 ($p = 855$ nm) 1.34 ± 0.3 (p=395nm)	0.9 ± 0.3 ($p = 855$ nm)	0.4 ± 0.25

4. TN and Grandjean structures with in-plane electric fields

4.1 Experiment

The experimental set up for the measurement of $(e_1 - e_3)$ using either an achiral TN or chiral Grandjean structure with an in-plane electric field is shown in Figure 2. The cells used have a 500μm planar gap etched into the layer of ITO on the lower substrate while the upper substrate has no ITO coating. Both substrates have a rubbed polymer homogeneous alignment layer and are assembled with 90° between the rubbing directions in a TN arrangement. The separation of the two substrates is engineered to be 10 μm using glass microspheres, so the aspect ratio of the electrode gap to cell thickness is 50:1.

As shown in Figure 2, the laser beams are incident on the device at ±45° to the substrate normal. If the beam is incident normally the tilt of the molecules due to the flexoelectro-optic effect is in opposite directions for electric fields $\pm E$, but these are optically equivalent and provide no information about the sign of $(e_1 - e_3)$ (see (*6*)). When observed at oblique incidence this degeneracy is lifted and the transmission is different for positive and negative voltages, revealing the direction of the flexoelectric tilt. Further the oblique transmission is more sensitive to the flexoelectric response if the molecular tilt is either towards or against the direction of propagation for the beams. The position of the laser beams within the device is observed via a CCD camera, to ensure that the beams are centred in the electrode gap and distant from any structural inhomogeneity.

The transmission of the laser beams through the centre of the electrode gap was measured as a function of voltage applied to the cell for the beam passing through crossed and parallel polarisers. The measurement was performed for azimuthal cell orientations of 0°, 45° and 90° between the electric field direction and the incident laser plane. The system is calibrated in the absence of the cell by inserting a 45° polariser between

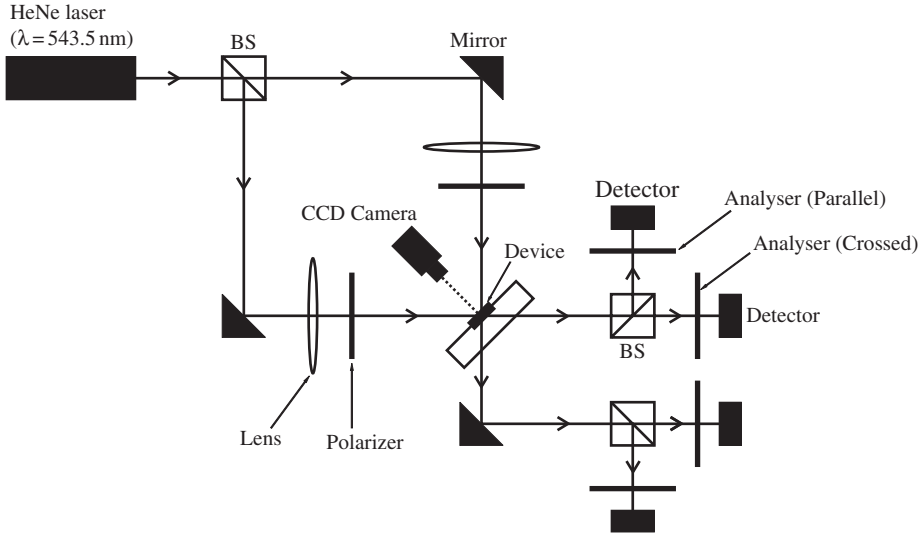

Figure 2. Experimental set up for the determination of $(e_1 - e_3)$ from the oblique transmission of two laser beams through a device aligned in the Grandjean structure with an applied in-plane electric field.

the initial polarisers and taking detector readings with and without the laser beam. This allows the normalised transmission to be calculated accurately taking into account detector offsets and beam-splitter and polariser inefficiencies.

The voltage applied was a square wave and the frequency chosen for each cell so as to have sufficient period for the transmission to reach equilibrium. The characteristic response time for the flexoelectro-optic effect can be estimated by considering the time for the tilt angle ϕ to relax back to zero on removal of the electric field and is found to be (*16*)

$$\tau = 2\gamma/(K_1 + K_3)q^2, \tag{5}$$

where γ is the effective viscosity for the rotation. The TN structure formed by the achiral materials has an effective pitch of four times the device thickness ($p \approx 40\ \mu m$). Such a long pitch material has a relatively long flexoelectric response time requiring the use of a quasi-dc driving frequency ($f = 0.2$ Hz). The measurements using the chiral Grandjean structure are only reported for the longer pitch materials (containing 1% R5011 chiral dopant w/w), and were performed for E7 and TL 216 at a frequency of 500 Hz which is in accordance with a calculation of τ. However, the measurements of MDA 02 2419 required a lower frequency of 25 Hz since the transmission took longer to reach equilibrium, possibly due to ionic motion in the device. The results for the shorter pitch materials (containing 2% R5011 w/w) in this set up are omitted since the angles of incidence for the laser beam on the devices ($\pm 45°$) were at a peak of the Bragg diffraction, causing a significant reduction in the accuracy of the measurement.

In order to determine a value of $(e_1 - e_3)$) from the experimental results, the transmission of the device is calculated theoretically and fitted to the data. Initially the equilibrium configuration of the director must be determined for each applied voltage, which can be achieved by minimising the free energy density of the system:

$$\begin{aligned} f(\hat{\mathbf{n}}) = {} & \frac{1}{2}K_1[\nabla \cdot \hat{\mathbf{n}}]^2 + \frac{1}{2}K_2[\hat{\mathbf{n}} \cdot (\nabla \times \hat{\mathbf{n}}) + q]^2 \\ & + \frac{1}{2}K_3[\hat{\mathbf{n}} \times (\nabla \times \hat{\mathbf{n}})]^2 - \frac{1}{2}\epsilon_0 \Delta\epsilon(\hat{\mathbf{n}} \cdot \mathbf{E})^2 \\ & - [e_1\hat{\mathbf{n}}(\nabla \cdot \hat{\mathbf{n}}) + e_3((\nabla \times \hat{\mathbf{n}}) \times \hat{\mathbf{n}}] \cdot \mathbf{E}, \end{aligned}$$

where the first three terms describe the Frank elastic energy for splay, twist and bend director deformations, while the fourth and fifth terms are related to the respective coupling of the dielectric and flexoelectric polarisation with the electric field. In the achiral TN arrangement an infinite pitch is assumed and so $q = 0$ in the twist elastic term. The free energy can be minimised by solving the Euler–Lagrange equations for each component of the director, which is carried out using a relaxation routine, with infinitely strong anchoring assumed at each substrate. It is known that both the zenithal and azimuthal anchoring strengths associated with PVA alignment are relatively high ($W_{\theta,\phi} \gtrsim 10^{-4}$ J m^{-2}) (*17*). The flexoelectric surface torque for both zenithal and azimuthal reorientation is expected to be more than an order of magnitude weaker than the surface torque, such that negligible surface reorientation is expected. The transmission through the subsequent minimum energy director profile is calculated using a Berremann 4×4 optics routine (*18*).

In the experiment the laser beams are focused down to a beam diameter of approximately 100 μm in the centre of the 500 μm electrode gap. Given that the device thickness is fixed to be about 10 μm, it is reasonable to assume in the simulation that the electric field is uniform and parallel to the substrates over the entire region probed by the beam. If the liquid crystal has the same dielectric constant as the glass, it can be shown that the electric field magnitude in the centre of the gap is given by $E = 2V/\pi g = 0.64V/g$ where V is the applied voltage and g is the electrode gap (*19*). In general the dielectric constant of liquid crystal materials tends to be greater than that of glass, so the electric field is concentrated in the gap to some extent leading to it having greater magnitude than calculated with the above relationship. The PVA alignment layer provides planar anchoring with a small pretilt ($\lesssim 1°$), and as such surface polarisation effects on the electric field magnitude are expected to be minimal. However, the magnitude of the electric field may also be affected by the motion of ion impurities in the liquid crystal. There can either be ionic screening leading to a reduction in the electric field or ionic injection from the electrode edges which can cause an enhancement of the field. Therefore, due to the uncertainty in the magnitude of the electric field, a scaling factor γ is incorporated into the simulation as $E = \gamma V/g$ and is varied in fitting the theoretical predictions to the experimental data.

At high frequencies, such as those used when taking data for the E7 and TL 216 Grandjean devices, ionic effects on the electric field should be small since the field direction is reversed before there is sufficient time for significant ion motion. For these devices the value of the scaling factor γ in fitting the experimental data to the theory is expected to be close to the lower limit of a uniform

dielectric ($\gamma = 2/\pi$)). Knowledge of the dielectric constants of the liquid crystal material and the glass substrates allow estimation of the degree to which the electric field is concentrated in the device, although the precise value of γ is difficult to determine analytically.

The response time of the chiral MDA 02 2419 Grandjean device was considerably longer than might be expected from Equation (5), which is likely due to ionic drift in the electrode gap altering the electric field before equilibrium is reached. At the frequency of 0.2 Hz used in measurements of the flexoelectric response in the achiral TN devices, the effects of ionic motion also need to be included since the time for migration across the electrode gap is calculated to be the same order of magnitude as the field period. Therefore, the scaling factor γ in the fitting to the theory of measurements on these devices is allowed to vary more freely, in order to take into account the effects of possible ionic screening and/or injection. Thus, the value of γ is assumed in the range $0.4 \lesssim \gamma \lesssim 1.1$.

4.2. *Results*

The experimental results for the transmission at oblique incidence through the electrode gap of the in-plane field Grandjean device containing E7 + 1% w/w R5011 are shown in Figure 3 for device orientations of 0°, 45° and 90° between the direction of the electric field and the incident laser plane. Asymmetry in the transmission between positive and negative voltages is observed since the flexoelectric tilt of the liquid crystal director planes with respect to the helix axis is proportional to the electric field, Equation (3). Therefore, the direction of the tilt reverses for positive and negative fields. The greatest asymmetry in the transmission is seen when the incident laser plane is at 90° to the electric field, as may be expected since the tilt of the molecules is in the plane perpendicular to the field and hence in the plane of the laser. Therefore, the direction of flexoelectric molecular tilt is either towards or against the propagation direction of the incident laser beams. When the electric field is in the same plane as the incident laser beam (cell orientation 0°), the asymmetry in transmission for $\pm V$

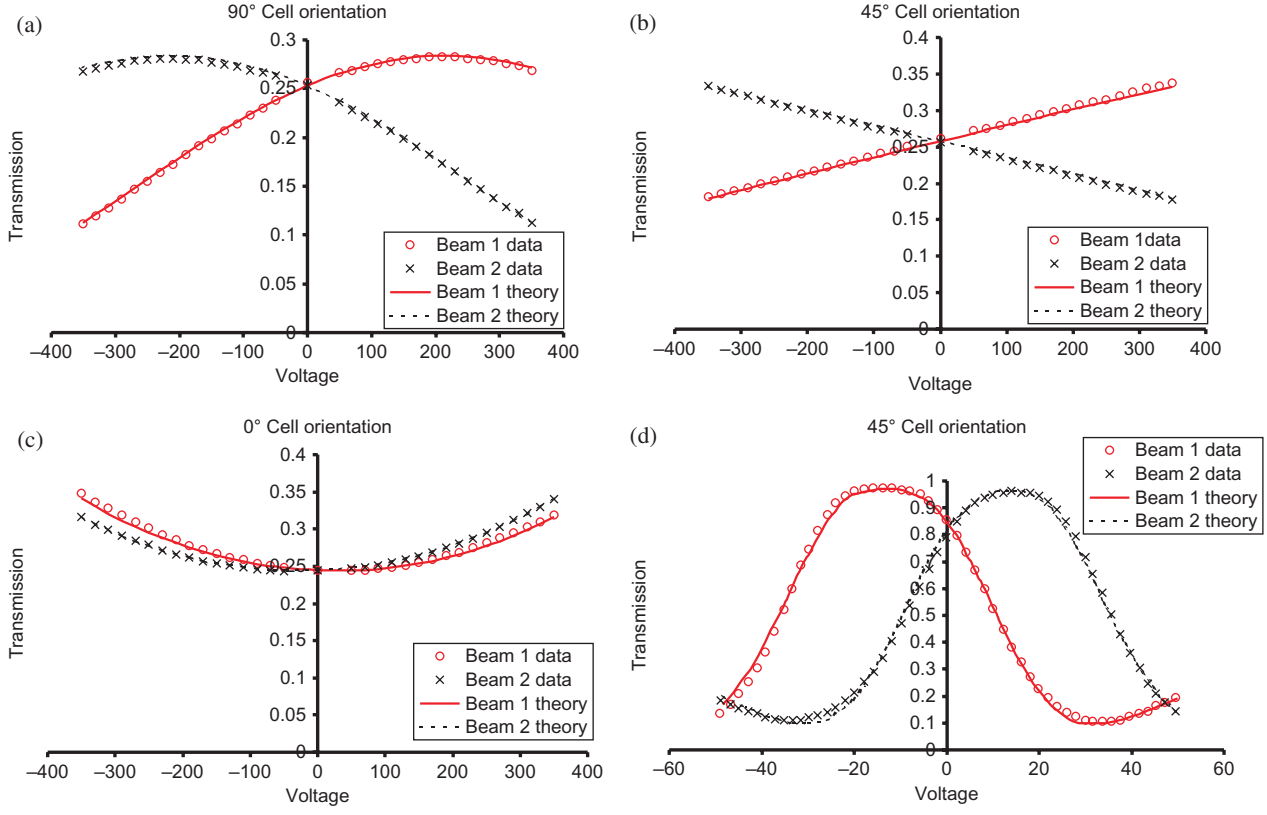

Figure 3. Experimental results for the oblique transmission through devices in the Grandjean/TN structure between crossed polarisers as a function of the applied in-plane voltage. Aligned in the Grandjean structure (E7 + 1% w/w R5011), three different device orientations are shown with (a) 90°, (b) 45° and (c) 0° between the electric field direction and the incident laser plane. (d) Data for pure E7 in the TN arrangement with 45° between the electric field direction and the laser plane. The two laser beams (1 and 2) are incident at ±45° to the cell normal. Also shown as solid lines are the best theoretical fits obtained for the data.

is lowest since the tilt of the molecules is out of the plane of incidence for the laser and appears similar for both voltage polarities.

Also shown in Figure 3(d) are the data for the achiral TN device containing E7 at an orientation of 45° between the electric field and incident laser plane. It can be seen that the flexoelectric response is far greater than in Figure 3(b) for E7 + 1% w/w R5011 in an identical setup but going to even higher applied voltage. This can be understood by considering Equation (3), which predicts that $\tan\phi \propto p$. The effective pitch is 40μm in the achiral TN, while the Grandjean device has a pitch of 825 nm, such that the flexoelectric tilt is expected to be approximately 50 times greater in the achiral TN for a given voltage.

When fitting the experimental data to the theoretical predictions from the model, the material parameters listed in Table 1 remain constant throughout. Initially the zero field transmission is used to determine the exact thickness of the liquid crystal layer for each device. The effect of a small pretilt in the surface alignment at each substrate is a disparity in the zero field transmission for the orthogonal laser beams, which is most pronounced in the achiral TN devices and included in the subsequent fitting. For the multi-turn Grandjean devices the influence of a small pretilt on the transmission is negligible and therefore omitted from the fitting process. In fitting the voltage dependence of the transmission data to the theory, the value of the flexoelectric difference $(e_1 - e_3)$ is allowed to vary freely, while the electric field scaling factor γ and the device orientation (angle between electric field and incident laser plane) vary within fixed limits. A change in the value of γ in the theory results in a scaling of the voltage axis, while modification of $(e_1 - e_3)$ alters the maximum and minimum values of the transmission, and hence the two effects are orthogonal (*12*).

It should be noted that the larger degree of flexoelectric response for the achiral TN structure, compared with that in the Grandjean structure (compare Figure 3(b) and (d)), aids the fitting process since there are more distinct features in the voltage-transmission curves with which to fix the fitting parameters. Determination of $(e_1 - e_3)$ in the Grandjean structure is initially carried out for a device orientation of 90° between the electric field and incident laser plane since this shows the greatest electro-optic response. Fitting of the transmission for device orientations of 45° and 0° is subsequently performed with identical values of $(e_1 - e_3)$ and γ to check consistency.

The theoretical curves shown in Figure 3 for E7 + 1% w/w R5011 with a pitch of 825 nm use the parameter values $(e_1 - e_3) = 12.2$ pC m^{-1} and $\gamma = 0.74$. The value for the electric field scaling factor is a little higher than the theoretical prediction for a uniform dielectric ($\gamma = 2/\pi = 0.637$), as expected since the higher dielectric constant of the liquid crystal layer relative to the glass causes a concentration in the field. The driving voltage is oscillating at a sufficiently high frequency (500 Hz) so that the field direction is expected to reverse before there can be any significant ionic influence on the field magnitude. The theoretical transmission shown in Figure 3(d) for pure E7 material in a TN device was calculated with parameters $(e_1 - e_3) = 12.2$ pC m^{-1} and $\gamma = 1.1$. Now the driving voltage is at a much lower frequency (0.2 Hz) and the effects of ions on the field magnitude are expected to be important. The increased value of the electric field scaling factor γ is attributed to ion injection at the electrode edges leading to an enhancement of the field.

For comparison it is interesting to consider the fitting of the theory to experimental data for TL 216, which is a material designed for use in TFT displays and as such has a low ionic content. Therefore, ionic perturbations to the field magnitude are expected to be negligible, even at low driving frequency. The best fit for the experimental data is achieved with values of $\gamma = 0.71$ at high frequency and $\gamma = 0.72$ at the quasi-dc frequency of 0.2 Hz. There is little difference between the two values confirming that any observed disparity between the high- and low-frequency values of γ is largely due to ionic motion. The values of γ are a little lower than the high-frequency Grandjean value for E7, reflecting a lesser degree of field concentration between the device substrates due to the lower average dielectric constant ($\bar{\epsilon} = 9.8$ for E7, while $\bar{\epsilon} = 5.7$ for TL 216). The fitting procedure for MDA 02 2419 yielded values of γ of 1.08 and 0.92 for measurements in the Grandjean and TN devices, respectively. MDA 02 2419 has the highest net dielectric constant ($\bar{\epsilon} = 20.9$), so the greatest degree of field concentration in the device is expected. Furthermore, the electro-optic response as a function of time after field reversal in both devices had an additional time constant distinct from flexoelectric and dielectric reorientations, indicating a significant ionic perturbation to the field magnitude, helping to justify the high values of γ.

The results for the measurements made on both the TN and Grandjean structures are collated in Table 2, combined with an estimation of the associated potential error. There is a degree of uncertainty in the transmission measurements, and also possible slight experimental misalignment. Additional error may arise due to uncertainty in the values of the material parameters, listed in Table 1, that are used in the theoretical model. The quoted error margin results from the range in flexoelectric values that provide a good fit to the

experimental data, taking into account these various uncertainties. It was stated above that infinitely strong surface anchoring was assumed at each substrate in the model when fitting the experimental measurements. It has been shown in a previous study on a similar system (*12*) that including a finite azimuthal surface anchoring ($W_\phi \sim 10^{-5}$ J m^{-2}) in the theory results in a modification in the value of $(e_1 - e_3)$ by around 5%. Therefore, given that the surface anchoring here is likely somewhat stronger ($W_\phi \sim 10^{-4}$ J m^{-2}), (*17*) the effects of any surface reorientation are expected to have minimal consequence on the values of $(e_1 - e_3)$ reported.

5. Conclusions

There is a good correlation observed for the results from the measurement of the flexoelectric difference for E7 in all three structures. For MDA 02 2419, the $(e_1 - e_3)$ values are very similar from measurements in the ULH and achiral TN structures. However there is some difference ($\gtrsim$20%) between these values and the value extracted for the chiral Grandjean structure, possibly influenced by the anomalous form of the flexoelectric response observed indicating a large amount of ionic contamination. The values of $(e_1 - e_3)$ for TL 216 show a little variation in absolute magnitude but are of the same order in each case. The low value of $(e_1 - e_3)$ for the material leads to difficulty in accurate measurement, especially for the chiral mixtures. For small tilt, ϕ is proportional to the pitch so for the short-pitch mixtures used only a very small tilt angle was obtainable ($\sim 1^\circ$ from ULH measurements and $\sim 0.1^\circ$ using the in-plane electric field). Such small flexoelctric tilt angles invoke only a small modulation in the transmitted intensity which is hard to measure precisely. There is a degree of error inherent in all of the measurements and it can be seen that the results for each material are consistent between the three structures within respective error margins.

The experiments show the equivalence of measured values for $(e_1 - e_3)$ obtained in the ULH, chiral Grandjean and achiral TN structures. It is demonstrated that observing the in-plane optic axis rotation for a highly chiral material in the ULH structure offers a quick and straightforward measurement of the flexoelectric difference without the need for any data fitting. However, monitoring the transmission through a device with helix axis perpendicular to the substrate and an in-plane electric field is seen to be the most generally applicable method. It has the advantage that it can be used for all materials including those that are naturally achiral or have a negative $\Delta\epsilon$ which are precluded form the ULH method. Further the liquid crystal structure required for the measurements is easy to align, removing the possibility of a badly aligned structure corrupting the results, and is also stable, enabling subsequent measurements on the identical texture. There are also advantages for using this method with highly chiral structures rather than the achiral TN since the device can be driven at high frequency while still observing a complete flexoelectric switch, reducing the problems associated with ionic motion in the electrode gap when trying to determine the electric field magnitude. However, the highly chiral structures have the drawback that the magnitude of the flexoelectric response is greatly reduced decreasing the accuracy of the experiment. The optimum structure for flexoelectric measurements in a standing helix geometry requires a compromise on the chiral pitch used: the pitch should be sufficiently short such that the liquid crystal response is much faster than any ionic response, but also long enough to exhibit a large flexoelectro-optic tilt.

More fundamentally, the experiment shows that the chirality of a material has little effect on its flexoelectric coefficients. This provides the first experimental verification that chirality, which is associated with a natural twist ($\hat{\mathbf{n}} \cdot (\nabla \times \hat{\mathbf{n}})$) of the director about the helical axis has no influence on flexoelectric behaviour, having been long predicted from symmetry considerations since there is no unique direction along which a polarisation might arise (*1*, *2*). The reason flexoelectricity is often studied in highly chiral systems, particularly in the flexoelectro-optic effect considered here, is that a lower mode of distortion is required to obtain a periodic bend–splay flexoelectric deformation than in an achiral nematic, as opposed to any enhancement of the flexoelectric coefficients.

Acknowledgments

The authors would like to thank Merck Chemicals Ltd and the EPSRC for financial and material support, and Daniel Corbett for useful discussion.

References

(1) Meyer, R.B. *Phys. Rev. Lett.* **1969**, *22*, 918–921.
(2) Rudquist, P.; Lagerwall, S.T. *Liq. Cryst.* **1997**, *23*, 503–510.
(3) Petrov, A.G. Measurements and interpretation of flexoelectricity. In *Physical Properties of Liquid Crystals: Nematics*, Dunmur, D.A., Fukuda, A. and Luckhurst, G.R. Eds; INSPEC, IEE: London, UK, 2001; pp. 251–264.

(4) Patel, J.S.; Meyer, R.B. *Phys. Rev. Lett.* **1987**, *58*, 1538–1540.
(5) Morris, S.M.; Castles, F.; Broughton, B.J.; Coles, H.J. *Proc. SPIE* **2007**, *6587*, 65871I.
(6) Broughton, B.J.; Clarke, M.J.; Blatch, A.E.; Coles, H.J. *J. Appl. Phys.* **2005**, *98*, 034109.
(7) Hubert, P.; Jägemalm, P.; Oldano, C.; Rajteri, M. *Phys. Rev. E* **1998**, *58*, 3264–3272.
(8) Rudquist, P.; Buivydas, M.; Komitov, L.; Lagerwall, S.T. *J. Appl. Phys.* **1994**, *76*, 7778–7783.
(9) Coles, H.J.; Musgrave, B.; Coles, M.J.; Willmott, J. *J. Mater. Chem.* **2001**, *11*, 2709–2716.
(10) Rudquist, P.; Komitov, L.; Lagerwall, S.T. *Liq. Cryst.* **1998**, *24*, 329–334.
(11) Coles, H.J.; Clarke, M.J.; Morris, S.M.; Broughton, B.J.; Blatch, A.E. *J. Appl. Phys.* **2006**, *99*, 034104.
(12) Ewings, R.A.; Kischka, C.; Parry-Jones, L.A.; Elston, S.J. *Phys. Rev. E* **2006**, *73*, 011713.
(13) Kischka, C.; Parry-Jones, L.A.; Elston, S.J.; Raynes, E.P. *Mol. Cryst. Liq. Cryst.* **2008**, *480*, 103–110.
(14) Kischka, C.; Parry-Jones, L.A.; Elston, S.J.; Raynes, E.P. Measurement of the Flexoelectric Coefficients e1 and e3 in Nematic Liquid Crystals. Presented at the 22nd BLCS conference, Norwich, UK, 17–19 March 2008.
(15) Lee, S.D.; Patel, J.S. *Phys. Rev. A* **1990**, *42*, 997–1000.
(16) Lee, S.D.; Patel, J.S.; Meyer, R.B. *J. Appl. Phys.* **1990**, *67*, 1293–1297.
(17) Oka, S.; Mitsumoto, T.; Kimura, M.; Akahane, T. *Phys. Rev. E* **2004**, *69*, 061711.
(18) Berreman, D.W. *J. Opt. Soc. Am.* **1972**, *62*, 502–510.
(19) Hallam, B.T.; Sambles, J.R. *Mol. Cryst. Liq. Cryst.* **2000**, *351*, 87–94.